INTERDIGITAL RF STRUCTURES

U. Ratzinger
GSI, P.O. 11 05 52, D-6100 Darmstadt, FRG

Abstract

The main advantage of the interdigital rf-structure is its shunt impedance which is outstanding especially at low particle energies.
During the last 4 decades several investigations with rf models were done to study the shunt impedance of cavities with interdigital structures and their suitability for the acceleration of protons and heavy ions. The "SchweIN" at the Munich Tandem Laboratory was the first IH-type cavity in use. It has postaccelerated heavy ions with q/A>0.3 from 2.4 MeV/u to 4.3 MeV/u since 1975. It is a short structure and does not contain any focusing elements, the velocity profile can be changed, the duty cycle is 100 %.
After the development of a special kind of beam dynamics it is now possible to combine tanks of the SchweIN-type to form a long linac.
Two-cavity combinations are in use at the Tandem laboratories in Munich and Roskilde, Denmark; one cavity is used at Tsukuba, Japan.
Recently there is a growing number of applications, where the structure is used to accelerate low energy beams. The Tokyo Institute of Technology built an IH structure with W=0.24 MeV/u - 2.4 MeV/u, using conventional beam dynamics and magnetic quadrupole focusing.
For the new 1.4 MeV/u injector at UNILAC/GSI, an IH-type cavity is under construction with innovations in beam dynamics and rf-structure.

Introduction

This article describes interdigital drift tube structures mounted inside a cavity and operated in the H_{111} mode. So far only room temperature devices exist.
Early studies of this structure on rf models were done around 1950 at several laboratories.
In 1956 J.P. Blewett mentioned some characteristics of that structure during his talk at the CERN-Symposium.[1] Some more detailed studies are reported in the Sixties from groups in the Soviet Union[2,3] and France[4,5].
In 1976 the first IH structure came to routine operation at the Munich MP Tandem Laboratory[6].
In the Eighties the application of this structure was extended to the acceleration of low energy Tandem beams at the Tokyo Institute of Technology[7] and to He^+- and N^+-beams out of a 40 kV plasma source at the FOM-Institute Amsterdam[8].

Geometry and field distribution

Fig. 1a shows the distribution of the electric and magnetic field lines inside a cylindrical cavity operated in the H_{111}-mode. By mounting the $\beta\lambda/2$-drift tube structure the resonance frequency is typically reduced by about 60 % of the original value (in case of the Alvarez structure the corresponding value is only 10 % - 20 %).
These numbers demonstrate that the effective capacity in case of the IH structure is very well concentrated at the drift tubes.

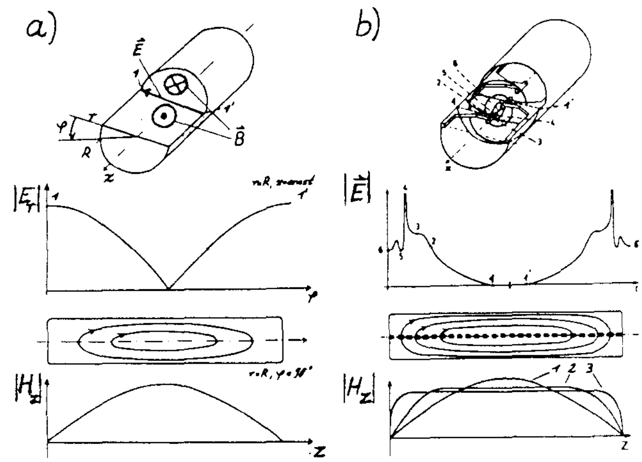

fig. 1a: Field distribution inside a cylindrical cavity, operated in the H_{111}-mode
b: Field distribution of the IH structure

One main problem to be solved was the flatness of the gap voltage distribution along the beam axis. It means to shift the magnetic field distribution from curve 1 of fig. 1b (capacity and inductivity per unit length of the cavity constant) to curve 3 (capacity and/or inductivity per unit length of the cavity increased towards the ends).
Figs. 2a and b show two ways of gap voltage flattening which provided good results and could stand cw operation:

- The Munich "f-SchweIN" cavity[6] consists of three parts. The middle part provides extended areas at the tank ends for the penetration of the magnetic field lines. The constant gap voltage distribution is additionally gained by variation of the gap length to cell length ratio g/L along the beam axis.
- The "second Tokyo tank" uses an optimized open end-type boundary to get a flat voltage distribution. By keeping the g/L-ratio constant the "E"-shaped magnetic-flux inducers at each side are matched to the velocity profile of the structure[7].

IH structures in operation

Table 1 shows a list of laboratories which use interdigital rf structures for the acceleration of heavy ions. The main characteristics of the different devices are mentioned in the last column.
Figs. 3 and 4 give an impression of the variety of realized geometries.

Efficient beam dynamics

As described above the effective resonator capacity C_R of the IH cavity is very well concentrated at the drift tube structure. At constant rf frequency, constant particle velocity and flexible tank dimensions the shunt impedance scales with $C_R^{-3/2}$.
At constant tank dimensions and constant particle

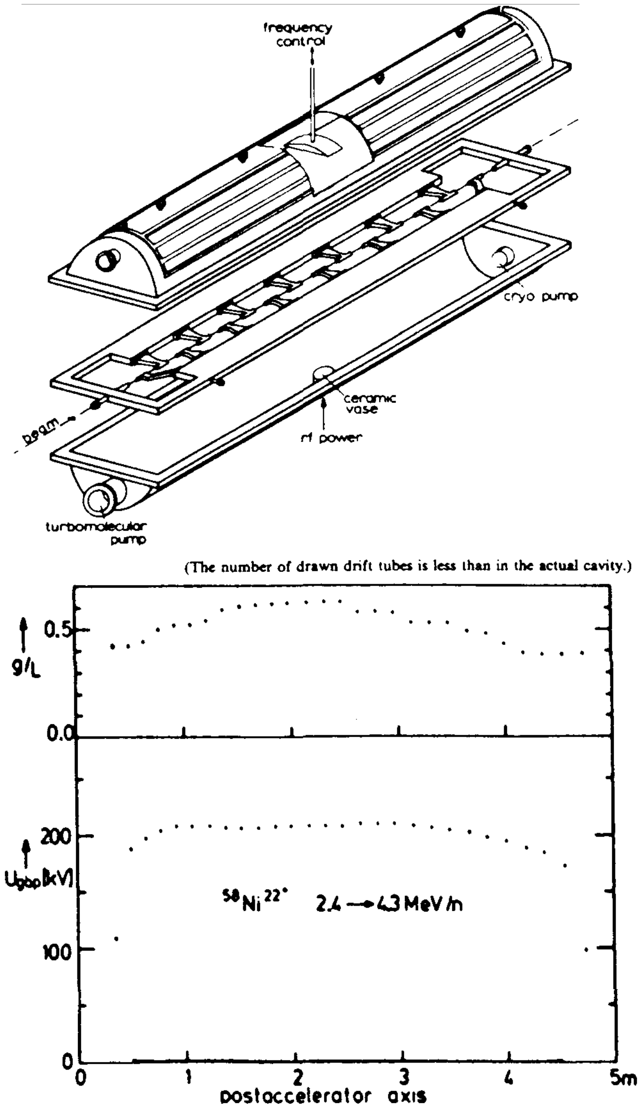

fig. 2a: Construction of the Munich "f-SchweIN" and flattening of the gap voltage distribution by variation of the g/L-ratio.

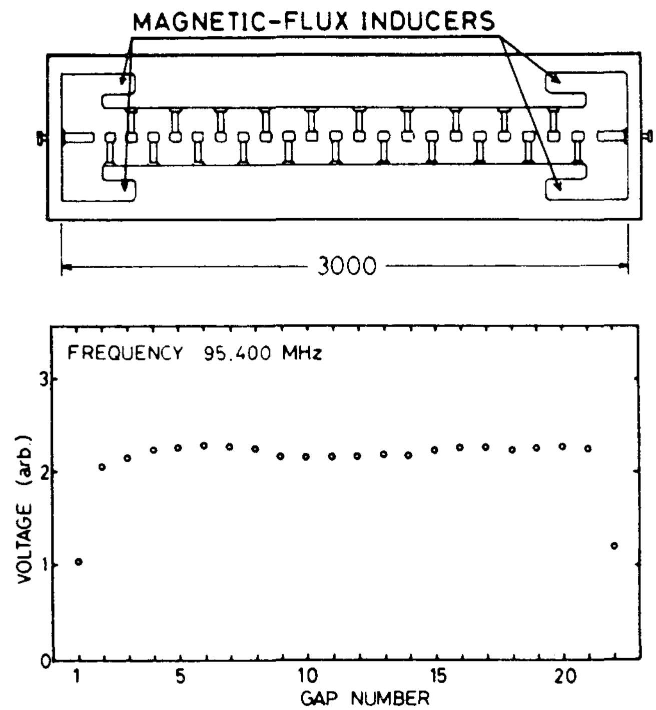

fig. 2b: The middle part of the Tokyo "2f-tank" and flattening of the gap voltage by "magnetic-flux inducers".

velocity the shunt impedance scales with $C_R^{-7/4}$ by varying the rf frequency.[8]
To achieve an optimum effective shunt impedance the drift tubes outer diameter should be as small as possible, that means construction of drift tubes without any quadrupoles or other space consuming focusing elements. This was the motivation to reduce the radial defocusing action of negative synchronous particle structures using ϕ_s=-30° typically.
A beam dynamics which accelerates the particle very close to the crest of the wave and has good transport capabilities in the 6-dim phase space was developed gradually in connection with the IH structure[9,10,11]. The theory was confirmed by experiment.
The main aspects of the "Beam dynamics of combined 0° synchronous particle structures" are summarized qualitatively below:

- Injection of the particle pulse at higher energy relative to the 0° synchronous particle (fig. 5). The excess energy Δ_0 of the pulse center at injection is related to the half axis δ_0 of the longitudinal beam emittance ($\Delta_0 = r \cdot \delta_0$: $1<r<1.5$ typically).
- In each 0° synchronous particle section the center particle of the pulse makes about one quarter phase oscillation around the synchronous particle. The energy-phase relation at the connection between neighbouring 0° synchronous particle sections can be seen from fig. 6. By that method it is possible to keep the position of the particle pulse mainly inside the second quadrant of the energy-phase plane providing a stable beam transport.
- The longitudinal focusing forces are concentrated near the end of each 0° synchronous particle section (position of the particles at negative rf phases). The motion of a single particle around the center particle of the pulse is shown qualitatively by fig. 7. Necessary conditions for cyclic motion are discussed in ref. 11.
- The transversal focusing of the beam is done at the end of each 0° synchronous particle section usually. This arrangement of longitudinal and transversal focusing provides a small beam diameter and allows for an accelerator construction with reduced apertures.

In case of low q/A-beams with big transversal emittance rebunching behind each lense by a short negative synchronous particle section may become necessary. An example is given in ref. 12, describing the IH structure for the new GSI injector[13].

Location		fr MHz	∅ m	L m	Z_{eff} MΩ/m	W_i MeV/u	W_f MeV/u	$(\frac{q}{A})$min		characteristics
Munich Tandem Laboratory Techn. Univ.	tank 1	78.5	1	5.0	150	2.4	4.3	0.34	φ_s = 0°	Injector: 12 MV-Tandem;
	tank 2	157	0.5+	3.0	150	4.3	6.0	0.40	- " -	quadrupole doublet between cavities;
Roskilde Niels Bohr Institute	tank 1	100	0.72	3.64	142	2.4	3.7	0.29	φ_s = 0°	Injector: 9 MV-Tandem;
	tank 2	100	0.72	3.64	105	3.7	4.9	0.29	- " -	quadrupole triplet between cavities; high reliability of operation;
Tsukuba University	tank 1	100.5	0.75	3.03	134	3.14	4.0	0.42	φ_s = 0°	Injector: 11 MV-Tandem; available rf power limited;
Tokyo Inst. of. Technology	tank 1	48	1.4	7.0	132	0.24	2.4	0.25	φ_s =-30°	Injector: 1.6 MV-Tandem;
	tank 2	96	0.76	3.0	130	2.4	3.4	0.25	φ_s = 0°	FODO quadrupole channel along tank 1;
Amsterdam FOM-Inst. & IAP,Ffm.	tank A	40	0.4	0.65	--	0.01	0.03	0.25	φ_s =-38°	MEQALAC, $^4He^+$,
	tank B	25	0.8+	1.7	~30	0.0028	0.071	0.07	φ_s =-30°...-42°,	4 beam channels, N^+, 0,56 mA;

+ := tank has no circular cross section

Table 1: IH structures used for heavy ion acceleration

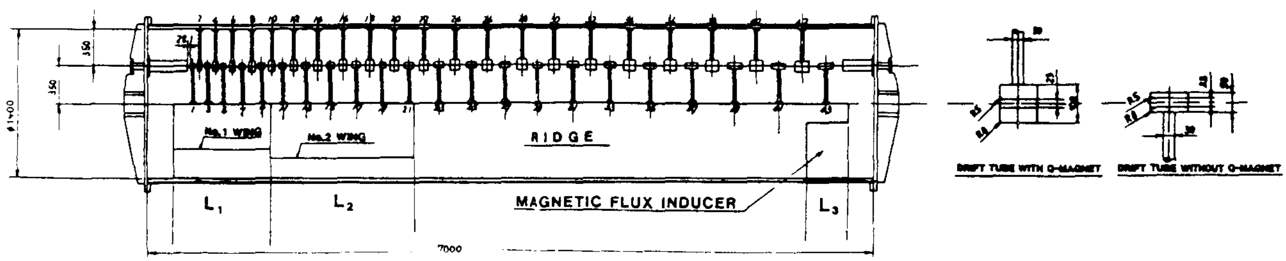

fig. 3: The Tokyo "f-tank".

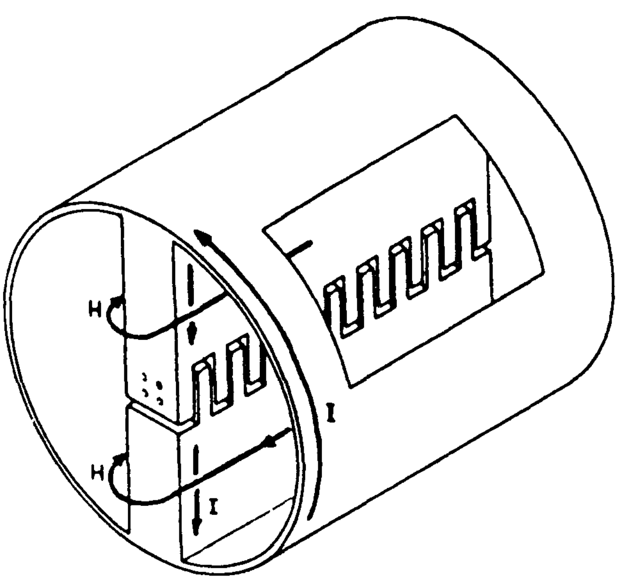

fig. 4: The Amsterdam "MEQALAC"-prototype, sketch[15].

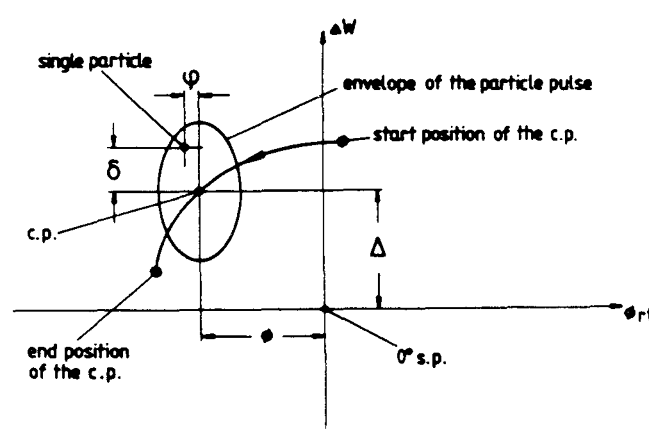

fig. 5: Motion of the particle pulse around the 0° synchronous particle in the longitudinal phase space.

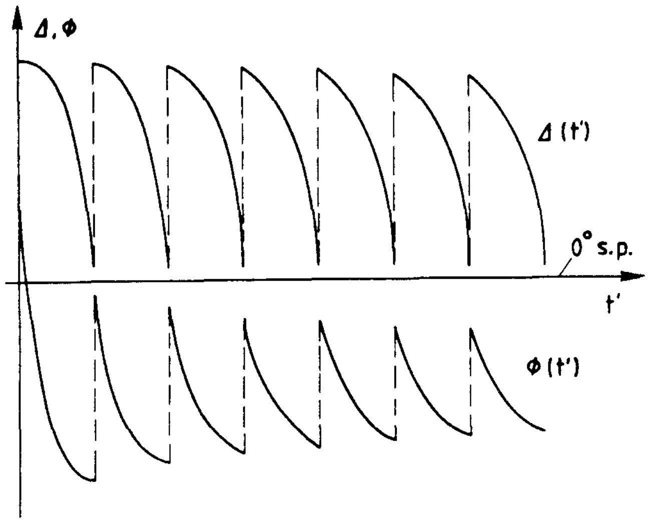

fig. 6: Position of the particle pulse center relative to the 0° synchronous particles of a long structure.

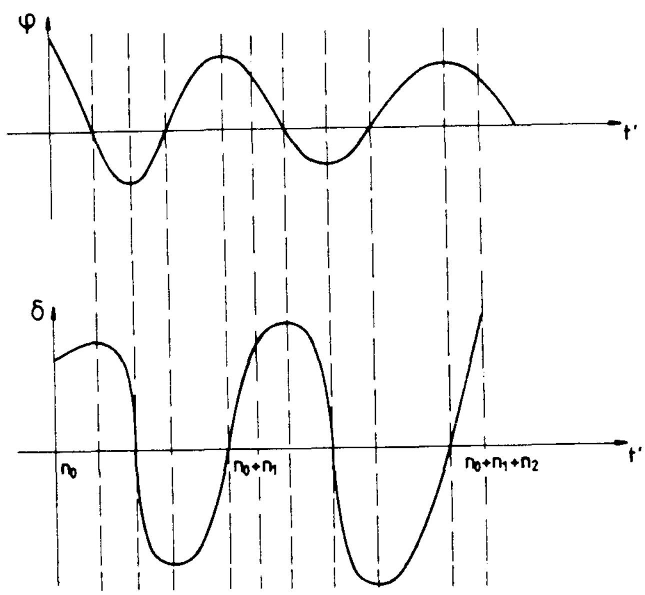

fig. 7: Oscillation of a single particle around the pulse center.

Improved drift tube geometry

To optimize the shunt impedance, the walls of the drift tubes and the capacitive ends of the stems should be thin; the inductive ends of the stems should be thick to get a low surface current density.
This procedure is limited by the electrical peak surface fields which are enhanced by reducing the outer diameter of the drift tubes. Another limit is the asymmetry of the gap field which is caused by the capacitive coupling between each drift tube and its neighboured stems (fig. 4 in ref. 10). This asymmetry grows when the capacitive coupling between the drift tubes is reduced.
By making use of thin walled drift tubes with a specific asymmetric shape (fig. 8), one can partly overcome the second limitation, which is serious especially for low energetic particles.

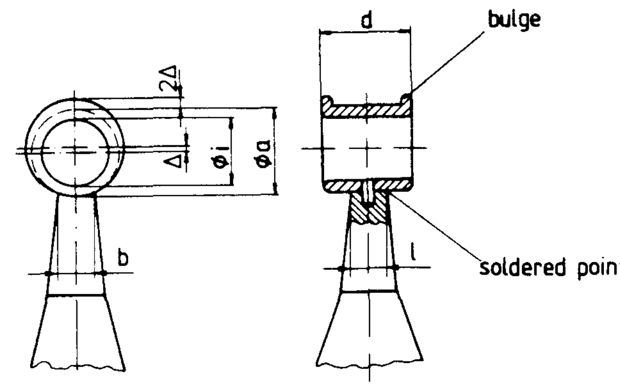

fig. 8: Dipole compensated drift tube geometry.

The advantage of the proposed geometry was confirmed qualitatively first by repeating the off axis perturbation measurements along some modified drift tubes at the GSI interdigital rf-model. Quantitative numerical results were obtained by using the 3-dim computer code PBM3D[14].
This program is solving Maxwell's equation of continuity:

$$\text{div}\left[(\kappa + i\omega_0\varepsilon_r) \cdot \text{grad } V\right] = 0;$$

κ: = electrical conductivity
V: = electrical potential

The code is based on the "method of differences" and can be used to find the field distribution of the capacitive part of a cavity with complicated geometry.
The voltage distribution along the stems is defined by their geometry and by κ. This distribution can be varied in a wide range without significant influence on the gap field distribution.
The tank walls are kept on zero potential.
The geometry used for the new GSI IH structure is shown in fig. 8. It is optimized to eliminate the dipole component at the low energy side.
The reduction of the dipole component at higher energies is shown in fig. 9.

Shuntimpedance

The efficiency of interdigital rf structures is shown by fig. 10. However additonally the normalized transversal acceptances $\alpha_n/\pi\cdot$mm mrad and $(q/A)_{min}$ have to be taken into account to compare with the UNILAC-structures:

Index in fig. 11:	1	2 + 3	4	5
α_n/π mm mrad	1.5	0.3	1	10
$(\frac{q}{A})_{min}$	0.11	0.3	0.04	0.11

Conclusions

Though the advantages of small size and very high shuntimpedance are known since about 40 years it took a long time to construct IH structures which allow for stable operation and high service load.
This structure is a very efficient tool for the acceleration of low energy beams up to about 20 Mev/u and q/A-values below one.
The dependence of the optimum rf frequency on the beam velocity is rather strong.

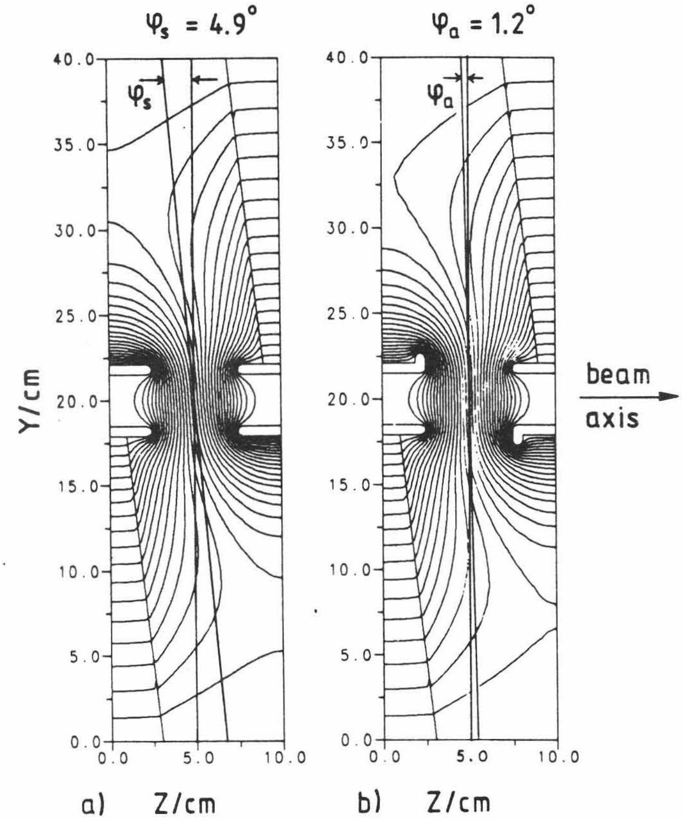

fig. 9: Influence of the bulges on the transverse electric field component.

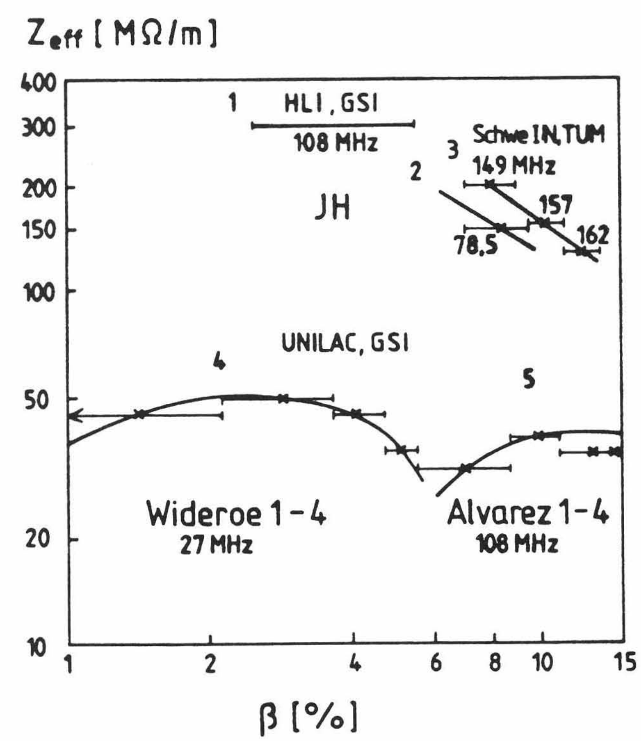

fig. 10: Comparison of shunt impedance and velocity range of several drift tube linacs

Acknowledgement

I like to thank Prof. H. Morinaga who was one of the very early pioneers to investigate the IH structure. He fortunately remembered to his former studies when he came to Munich and provided an interesting field of activity to many of his students.

References

[1] J.P. Blewett, Linear accelerator injector for proton synchrotrons, CERN symposium (1956), 162.

[2] P.M. Zeidlitz, V.A. Yamnitskii, Accelerating systems employing H-type waves, Plasma Physics (Journal of Nucl. Energy, Part C), Vol. 4 (1962), 121.

[3] V.A. Bomko, E.I. Revutskii, L.I. Bolotin, High frequency characteristics of a linear accelerator raising multicharge ions to energies of 1 MeV per nucleon in an H_{111} wave, Soviet Physics Techn. Physics, 9 (1965), 977.

[4] J. Pottier, A new structure for heavy ion linacs, IEEE Trans. Nucl. Sci. Vol. NS-16/3 (1969), 377.

[5] M. Bres, A. Chabert, J.-C. Gavet, D.T. Tron, B. Veyron, G. Voisin, Study on interdigital H-Type structure for heavy ion linear accelerator, IEEE Trans. Nucl. Sci., Vol. NS-16/3 (1969), 372.

[6] E. Nolte, G. Geschonke, K. Berdermann, R. Oberschmid, R. Zierl, M. Feil, A. Jahnke, M. Kress and H. Morinaga, The Munich heavy ion postaccelerator, Nucl. Instr. and Meth. 158 (1979), 311.

[7] K. Satoh, T. Mitsumoto and E. Arai, Construction and operating experience with the Tokyo Institute of Technology post accelerators, Nucl. Instr. and Meth. A 268 (1988), 538.

[8] E. Nolte, R. Geier, W. Schollmeier and S. Gustavsson, Improved performance of the Munich heavy ion postaccelerator, Nucl. Instsr. and Meth. A 201 (1982), 281.

[9] U. Ratzinger, R. Geier, W. Schollmeir, S. Gustavsson and E. Nolte, The three-harmonics double-drift buncher at the Munich heavy ion postaccelerator, Nucl. Instr. and Meth. 205 (1983), 381.

[10] U. Ratzinger, E. Nolte, R. Geier, N. Gärtner and H. Morinaga, The upgraded Munich heavy ion postaccelerator, Nucl. Instr. and Meth. A 263 (1988), 261.

[11] U. Ratzinger and U. Blell, Acceleration of low energy heavy ion beams with the IH structure, to be published in Nucl. Instr. and Meth.

[12] U. Ratzinger, A low beta rf linac-structure of the IH-type with improved radial acceptance, proc. of 1988 Linac Conf., CEBAF-rep. 89-001 (1989), 185.

[13] N. Angert, L. Dahl, J. Glatz, J. Klabunde, M. Müller, U. Ratzinger, B. Wofl, H. Deitinghoff, J. Friedrich, H. Klein, A. Schempp, A new 1.4 MeV/u injector Linac for the UNILAC, these proceedings.

[14] Computer code PB M3D for the calculation of electrical fields with capacitive and ohmice components. Author U. Blell

[15] J.G. Bannenberg, W.H. Urbanus, R.G.C. Wojke, H. Klein, R.W. Thomae, A. Schempp, T. Weis, P.W. van Amersfoort, MEQALAC: A1 MeV multichannel rf accelerator for nitrogen ions, these proceedings.